

# The Effect of Cracks on the Free Vibration of a Plate with Parabolic Thickness

**Vinh An Le**

Faculty of Civil Engineering, University of Transport and Communications, Vietnam  
levinhan@utc.edu.vn

**Xuan Tung Nguyen**

Faculty of Civil Engineering, University of Transport and Communications, Vietnam  
ngxuantung@utc.edu.vn (corresponding author)

Received: 7 April 2023 | Revised: 29 April 2023 and 13 May 2023 | Accepted: 17 May 2023

Licensed under a CC-BY 4.0 license | Copyright (c) by the authors | DOI: <https://doi.org/10.48084/etasr.5923>

## ABSTRACT

This paper uses first-order shear deformation theory and the finite element method to analyze the vibrations of rectangular plates with one or more cracks. The study investigated the influence of cracks (length, angle of inclination), the number of cracks, and the ratio of plate thickness to the natural vibration frequency of the plate, using phase field simulation. Plate thickness varies nonlinearly with the parabolic function. The results of the proposed method were compared with reputable studies to verify its reliability. In addition, some pictures of the characteristic vibration patterns of the plate with varying thickness are presented when cracks appear.

**Keywords**-cracked plate; free vibration; phase field; variable thickness

## I. INTRODUCTION

Plates with variable thicknesses are often used when aesthetic elements are needed to ensure the bearing capacity of a structure. In [1], the vibration frequency of orthogonal nanoplates with variable thickness was explored using Eringen's theory combined with the nonlocal classical plate theory. In [2], the vibration frequency and bending load of a rectangular multilevel plate were calculated based on the classical plate theory (Kirchhoff). In [3], the free oscillation of a variable thickness plate was analyzed using first-order shear deformation and the higher-order shear deformation plate theories. In [4], the Frobenius method was used to determine the buckling load for an elastic rectangular plate with variations in thickness, elastic modulus, and density. In [5], the two-variable refined plate theory and the Hamilton principle were used to calculate the free vibration frequencies of orthogonal plates. In [6], a general integral transformation technique was used to study the flexural resistance of rectangular plates with linearly variable thickness lying on a Pasternak elastic foundation. Structural plates are used quite frequently in fields such as mechanical engineering, construction, etc. During its lifetime, the plate may develop cracks due to local damage. To determine the degree of damage, it is necessary to re-evaluate the working capacity of the structure at that time. Scientists have proposed several theories and research methods on this issue, such as isogeometric analysis (IGA), finite element method (FEM), extended finite element method (XFEM), etc. In [7-8], FEM and stochastic high-order FEM were applied to analyze a continuous beam. In [9], an analytical solution was

used to dynamically analyze a functionally graded plate. More recently, in [10-16], the Phase-Field theory and FEM were used to analyze the stability and free vibration of a cracked rectangular plate.

To the best of our knowledge, no study has investigated the free oscillation of cracked plates with varying parabolic thickness. This study focused on calculating the vibration frequency parameter of a plate depending on the ratio of the plate edges, the length and angle of crack inclination, and the number of cracks.

## II. ESTABLISHMENT OF EQUATIONS

Using Reissner-Mindlin first-order shear deformation plate theory, the displacement in the mid-plate section is given by:

$$\begin{aligned}\tilde{u}(x, y, z, t) &= u_0(x, y, t) + z\theta_x(x, y, t) \\ \tilde{v}(x, y, z, t) &= v_0(x, y, t) + z\theta_y(x, y, t) \\ \tilde{w}(x, y, z, t) &= w_0(x, y, t)\end{aligned}\quad (1)$$

where  $\tilde{u}$ ,  $\tilde{v}$ ,  $\tilde{w}$  are displacements at any point along the  $x$ ,  $y$ , and  $z$  axes, respectively,  $\theta_x$  and  $\theta_y$  are rotation angles in the  $xz$  and  $yz$  faces, and  $u_0$ ,  $v_0$ , and  $w_0$  are the displacements at the center of the plate. The deformation components of are given by:

$$\begin{Bmatrix} \varepsilon \\ \gamma \end{Bmatrix} = \begin{Bmatrix} \varepsilon_p \\ 0 \end{Bmatrix} + \begin{Bmatrix} Z\varepsilon_b \\ \gamma_s \end{Bmatrix}\quad (2)$$

where:

$$\begin{aligned} \varepsilon_p &= \begin{Bmatrix} u_{0,x} \\ v_{0,y} \\ u_{0,y} + v_{0,x} \end{Bmatrix} \\ \varepsilon_b &= \begin{Bmatrix} \theta_{x,x} \\ \theta_{y,y} \\ \theta_{x,y} + \theta_{y,x} \end{Bmatrix} \\ \gamma_s &= \begin{Bmatrix} \theta_x + w_{0,x} \\ \theta_y + w_{0,y} \end{Bmatrix} \end{aligned} \quad (3)$$

The relationship between stress and strain is:

$$\begin{Bmatrix} \sigma \\ \tau \end{Bmatrix} = \begin{bmatrix} D_m & 0 \\ 0 & D_s \end{bmatrix} \begin{Bmatrix} \varepsilon \\ \gamma \end{Bmatrix} \quad (4)$$

and the strain energy in the plate is expressed by:

$$\Pi(\delta) = \frac{1}{2} \int_{\Omega} \left\{ \varepsilon_p^T A \varepsilon_p + \varepsilon_b^T B \varepsilon_b + \varepsilon_b^T B \varepsilon_p + \varepsilon_b^T D \varepsilon_b + \gamma_s^T D_s \gamma_s \right\} d\Omega \quad (5)$$

where:

$$D_m = \frac{E}{1-\nu^2} \begin{bmatrix} 1 & \nu & 0 \\ \nu & 1 & 0 \\ 0 & 0 & (1-\nu)/2 \end{bmatrix} \quad (6)$$

$$D_s = \frac{kEh}{2(1+\nu)} \begin{bmatrix} 1 & 0 \\ 0 & 1 \end{bmatrix} \quad (7)$$

and:

$$(A, B, D_b) = \int_{-h/2}^{h/2} (1, z, z^2) D_m dz \quad (8)$$

with  $k$  being the shear correction factor.

In phase field theory, the variable  $s$  represents the deterioration of the material when the plate cracks [7-13]. It takes the value 0 when fully cracked and 1 when the material is in its normal state. Values of  $s$  from 0 to 1 represent the fracture zone of the material, where the object changes continuously from normal ( $s = 1$ ) to complete cracking ( $s = 0$ ). The deformation energy when the plate has cracks is given by:

$$\Pi(\delta, s) = \left\{ \begin{aligned} & \frac{1}{2} \int_{\Omega} s^2 \left\{ \varepsilon_p^T A \varepsilon_p + \varepsilon_b^T B \varepsilon_b + \varepsilon_b^T B \varepsilon_p + \varepsilon_b^T D \varepsilon_b + \gamma_s^T D_s \gamma_s \right\} d\Omega \\ & + \int_{\Omega} G_c h \left[ \frac{(1-s)^2}{4l_c} + l_c |\nabla s|^2 \right] d\Omega \end{aligned} \right\} = \left\{ \int_{\Omega} s^2 \Phi(\delta) d\Omega + \int_{\Omega} G_c h \left[ \frac{(1-s)^2}{4l_c} + l_c |\nabla s|^2 \right] d\Omega \right\} \quad (9)$$

where  $s$  simulates the state of the material,  $l_c$  is the crack width,  $G_c$  is the energy release rate, and  $\delta$  is the displacement vector. The kinetic energy of the plate is determined by:

$$W^e = \frac{1}{2} \int_{\Omega_e} s^2 \dot{u}^T \rho \dot{u} d\Omega = \frac{1}{2} \dot{\delta}^T M^e \dot{\delta} \quad (10)$$

The Lagrange function is calculated according to:

$$L(\delta, s) = W(\delta, s) - \Pi(\delta, s) \quad (11)$$

$$L(\delta, s) = \int_{\Omega} \left\{ s^2 \Psi(\delta) - G_c h \left[ \frac{(1-s)^2}{4l_c} + l_c |\nabla s|^2 \right] \right\} d\Omega \quad (12)$$

After taking the variation of  $L(\delta, s)$  in terms of  $\delta$  and  $s$ , a system of equations is used to determine the frequency of free vibrations of the cracked plate:

$$\left\{ \begin{aligned} & (\sum K^e + \omega^2 \sum M^e) \delta = 0 \\ & \int_{\Omega} \left\{ 2s \Psi(\delta) \delta s - 2G_c h \left[ -\frac{(1-s)\delta s}{4l_c} + l_c \nabla s \nabla(\delta s) \right] \right\} d\Omega = 0 \end{aligned} \right. \quad (13)$$

After solving the system of (13) the free vibration frequency of the cracked plate will be found. In this part, the finite element used is a triangular element with a function of the form:

$$N_i = \{1xy\} \begin{Bmatrix} a_i \\ b_i \\ c_i \end{Bmatrix}$$

with:

$$a_i = \frac{(x_j y_k - x_k y_j)}{(2\Omega_e)}$$

$$b_i = \frac{(y_j - y_k)}{(2\Omega_e)}$$

$$c_i = (x_k - x_j) / (2\Omega_e)$$

The element stiffness matrix is:

$$K^e = \int_{\Omega_e} h B_d^T D B_d d\Omega = h \Omega_e B_d^T D B_d$$

with the deformation matrix-node displacement of the element:

$$B_d = \begin{Bmatrix} a_1 & 0 & a_2 & 0 & a_3 & 0 \\ 0 & b_1 & 0 & b_2 & 0 & b_3 \\ b_1 & a_1 & b_2 & a_2 & b_3 & a_3 \end{Bmatrix}$$

The element Mass Matrix is:

$$M^e = \int_{\Omega_e} h N^T \rho N d\Omega$$

$$N = \begin{Bmatrix} N_1 & 0 & N_2 & 0 & N_3 & 0 \\ 0 & N_1 & 0 & N_2 & 0 & N_3 \end{Bmatrix}$$

Figure 1 shows the triangular element with area  $\Omega_e$  and vertices 1( $x_1, y_1$ ), 2( $x_2, y_2$ ), and 3( $x_3, y_3$ ).

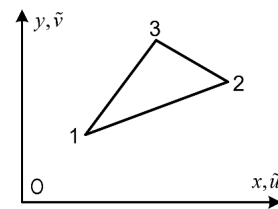


Fig. 1. The triangular element of plate.

### III. NUMERICAL RESULTS

#### A. Comparison of the Free Oscillations of the Parabolic Thickness Plate

The free oscillation of the parabolic thickness plate was calculated and compared with [3]. The plate is made of steel (SUS304), whose elastic modulus, mass density, and Poisson coefficient are  $E = 201.04$  GPa,  $\rho = 8166$  kg/m<sup>3</sup>, and  $\nu = 0.3$ , respectively. Figure 2 shows the thickness of the plate, which varies along the  $x$  direction with a quadratic rule:

$$h(x) = h_0(\mu \xi^2 - 2\mu \xi + 1), \mu = 1 - h_a/h_0$$

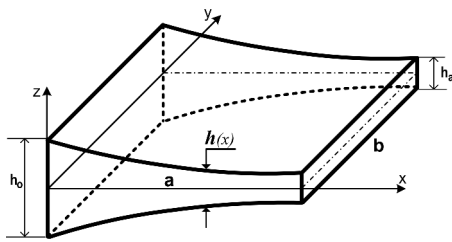


Fig. 2. Rectangular plate with parabolic variable thickness.

The square plate has side dimensions  $a = b = 0.5$  m. The natural vibration frequency of the plate is calculated by [14]:

$$\tilde{\omega} = \omega b^2 \sqrt{\rho h_0 / D_0} / \pi^2 \quad (14)$$

where:

$$D_0 = E h_0^3 / (12(1 - \nu^2))$$

Table I shows the frequency of the plate with different thickness ratios and boundary conditions of the four-sided mount. It can be seen that the difference between this study and [3] is very small, demonstrating the reliability of the method.

TABLE I. FREE OSCILLATION FREQUENCY OF PLATE WITH VARYING PARABOLIC THICKNESS

M	$h_0/a$	[3]	This study	Diff. (%)
0.25	0.1	2.8316	2.83135	-0.01%
	0.2	2.4311	2.42521	-0.24%
	0.3	2.0533	2.03532	-0.88%
	0.4	1.7503	1.71872	-1.80%
0.5	0.1	2.2850	2.2846	-0.02%
	0.2	2.0573	2.05506	-0.11%
	0.3	1.8090	1.80115	-0.43%
	0.4	1.5870	1.57104	-1.01%

B. Comparison of the Free Oscillations of a Constant-Thickness Plate with a Central Crack

The vibration of a cracked plate with constant thickness was found and compared with [17]. Figure 3 shows the crack in the center of the plate with length  $c$  and angle of inclination  $\alpha$ . The plate was made of ceramic  $Al_2O_3$ , with elastic modulus, density, and Poisson coefficient of  $E_c = 380$  GPa,  $\rho_c = 3800$  kg/m<sup>3</sup>, and  $\nu = 0.3$ , respectively. The square plate has a single support boundary condition on the four sides (SSSS), side dimensions  $a = b = 0.5$  m, and sheet thickness  $h = a/50$ . The free oscillation frequency is calculated according to [15]:

$$\hat{\omega} = \omega (b^2/h) \sqrt{\rho_c/E_c} \quad (15)$$

Table II shows that the difference between the proposed method and [17] (three-dimensional elasticity theory and Ritz method) or [12] (high-order shear deformation theory) is very small.

TABLE II. FREQUENCY OF CONSTANT THICKNESS PLATE WITH A CRACK

$c/a$	[17]	[12]	This study	Max Diff (%)
0	5.965	5.96947	5.96961	0.08%
0.1	5.939	5.92339	5.92562	-0.23%
0.3	5.665	5.71588	5.71592	0.90%
0.5	5.318	5.34453	5.34569	0.52%

C. Free Oscillation of a Single-Crack Plate with Parabolic Thickness Variation

The properties of the material and the dimensions of the plate are the same as in A. The plate had a crack with length  $c$  in the middle, and an angle  $\alpha$  between the crack and the  $x$ -axis, as shown in Figure 3. The frequency of the plate was calculated with (14). This plate had a single support boundary condition on four sides (SSSS) and a thickness of  $h_0 = 0.005$  m. Table III shows the frequency for the square plate with  $a = b = 0.5$  m and a thickness ratio of  $h_d/h_0 = 0.5$ . Table III shows that as the length of the crack increases, the stiffness of the plate decreases, leading to a decrease in the free vibration frequency. This is also shown in Tables IV, V, and VI. As the crack inclination angle  $\alpha$  increases, the frequency increases (a relatively small amount) until an angle of  $75^\circ$  and then decreases at  $90^\circ$ . Figure 4 shows that the natural frequency decreases with increasing thickness index and plate edge ratio ( $a/b$ ). As the thickness ratio decreases, the plate becomes thinner at the side parallel to the  $y$ -axis, causing the plate stiffness to decrease, leading to a corresponding decrease in frequency.

TABLE III. FREQUENCY OF THE PLATE DEPENDING ON CRACK LENGTH AND ANGLE.

Crack angle	$c/a$				
	0	0.1	0.3	0.5	0.7
$0^\circ$	1.31854	1.31116	1.29279	1.2672	1.23825
$15^\circ$	1.31854	1.31119	1.29276	1.26679	1.23688
$30^\circ$	1.31854	1.31127	1.29278	1.26604	1.23426
$45^\circ$	1.31854	1.31141	1.29302	1.26604	1.23412
$60^\circ$	1.31854	1.31158	1.29372	1.26726	1.2358
$75^\circ$	1.31854	1.31854	1.29519	1.2716	1.24469
$90^\circ$	1.31854	1.31173	1.29425	1.26893	1.23899

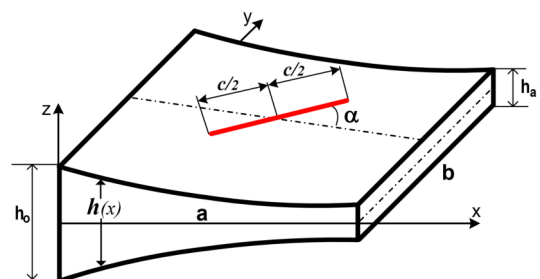


Fig. 3. The cracked plate with parabolic thickness.

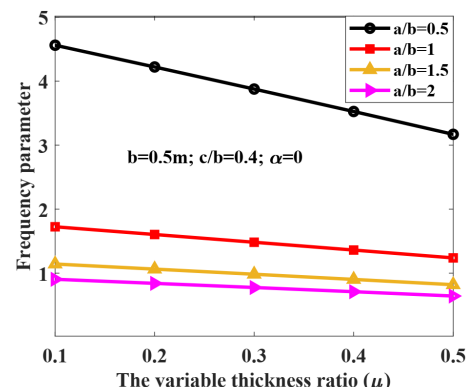


Fig. 4. The relationship between frequency and plate thickness index.

Table IV shows the frequency of the plate depending on the edge ratio, thickness ratio, and crack length. The crack inclination angle is  $\alpha = 0$ , i.e., the crack is parallel to the  $x$ -axis. With  $b = 0.5$  m, as the aspect ratio  $a/b$  increases, the mass of the plate increases, and as the frequency of vibration is inversely proportional to the mass, leads to a decrease in the frequency of vibrations. Figure 5 shows the first four vibration patterns of the cracked plate with parabolic thickness, with parameters values  $h_0 = 0.005$  m,  $a = b = 0.5$  m,  $h_d/h_0 = 0.6$ ,  $c/b = 0.5$ , and  $\alpha = 0^\circ$ .

TABLE IV. EFFECT OF EDGE RATIO AND THICKNESS RATIO ON FREQUENCY OF CRACKED PLATE

c/a	a/b	h <sub>d</sub> /h <sub>0</sub>				
		0.9	0.8	0.7	0.6	0.5
0	0.5	4.65504	4.30576	3.95052	3.58864	3.21947
	1	1.86601	1.73149	1.59556	1.45801	1.31854
	1.5	1.34604	1.24703	1.14624	1.04326	0.93746
	2	1.16278	1.07465	0.98408	0.89053	0.79326
0.2	0.5	4.62233	4.27621	3.92457	3.56684	3.20244
	1	1.81979	1.68984	1.5588	1.42652	1.29279
	1.5	1.2765	1.18422	1.09059	0.99529	0.89778
	2	1.06977	0.9906	0.9097	0.82666	0.74079
0.4	0.5	4.56125	4.22142	3.87646	3.52585	3.16907
	1	1.72443	1.60394	1.4828	1.36095	1.23825
	1.5	1.14271	1.06326	0.98308	0.90196	0.81948
	2	0.90419	0.84051	0.77593	0.71018	0.64277
0.6	0.5	4.4955	4.16295	3.82544	3.48241	3.13333
	1	1.62882	1.51802	1.40684	1.29527	1.18319
	1.5	1.02176	0.954	0.88588	0.81721	0.74767
	2	0.76769	0.7168	0.6654	0.61326	0.55999

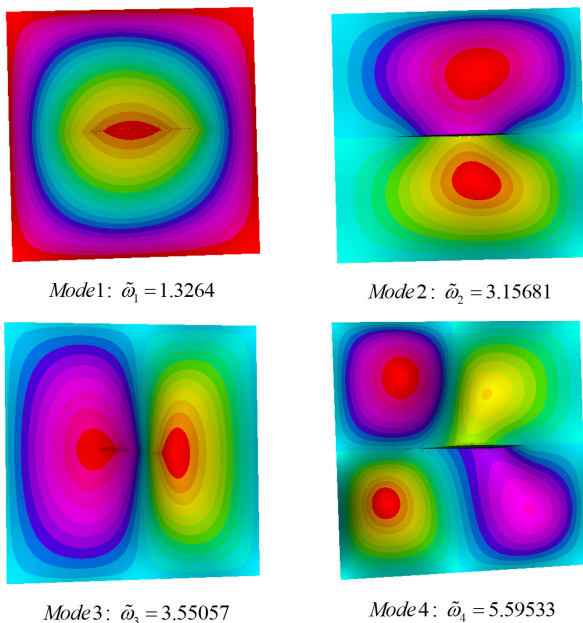


Fig. 5. The first four vibrations of the cracked plate.

D. Free Oscillation of a Multi-Cracked Plate with a Parabolic Variation of Plate Thickness

Figure 6 shows a plate with parabolic thickness and 3 cracks parallel to the  $y$ -axis. Table V shows the frequency versus the number of cracks, crack length, and the distance

between cracks. The ratios of the plate thickness and the two plate sides remain  $h_d/h_0 = 0.6$  and  $a/b = 0.6$ . For two cracks, when the crack length is small, i.e.  $c/b = 0.2$  or  $c/b = 0.4$ , increasing the distance between them ( $d$ ) will increase the frequency; conversely, with a crack length greater than  $0.6b$ , the frequency decreases. This is explained by the different energy released by the parabolic plate thickness. Figure 7 shows the first four vibration patterns of a plate with two cracks parallel to the  $y$ -axis and  $h_0 = 0.005$  m,  $a = b = 0.5$  m,  $h_d/h_0 = 0.4$ ,  $c/b = 0.6$ , and  $d = 0.25a$ .

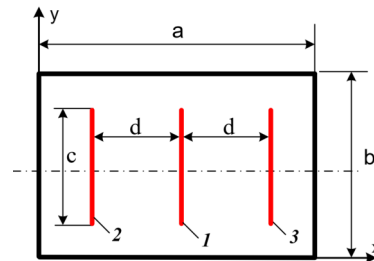


Fig. 6. The parabolic thickness plate with three cracks.

TABLE V. FREQUENCY OF A PLATE WITH MANY CRACKS

Number of cracks	c/b	d/a			
		0.1	0.2	0.3	0.4
1	0.2	1.03342	1.03342	1.03342	1.03342
	0.4	1.01087	1.01087	1.01087	1.01087
	0.6	0.984192	0.984192	0.984192	0.984192
	0.8	0.962094	0.962094	0.962094	0.962094
2	0.2	1.02582	1.02822	1.03341	1.03917
	0.4	0.990864	0.992979	1.00401	1.01917
	0.6	0.952778	0.948374	0.957069	0.974258
	0.8	0.918942	0.905287	0.905997	0.914716
3	0.2	1.02128	1.02058	1.0246	1.02968
	0.4	0.985226	0.976855	0.98136	0.991659
	0.6	0.948196	0.928833	0.926322	0.93481
	0.8	0.913994	0.883802	0.872667	0.874046

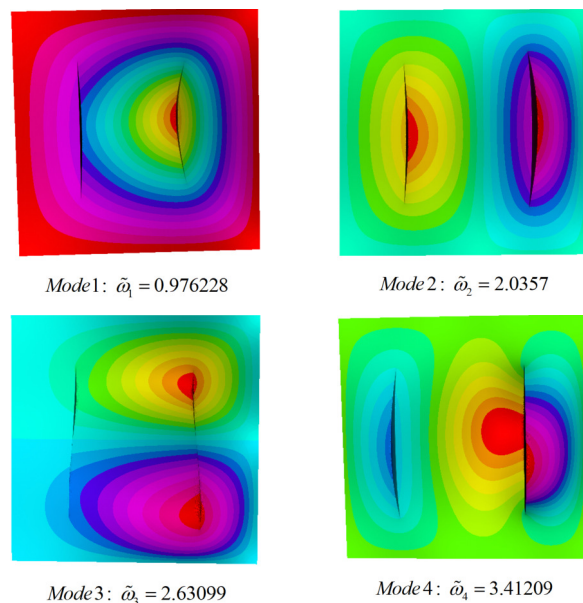


Fig. 7. First four oscillations of parabolic thickness plate with 2 cracks.

Table VI shows the frequency of a plate with three cracks depending on the thickness index and constant ratio of the two sides and distance between the cracks  $a/b = 1.25$ ,  $d/a = 0.25$ .

TABLE VI. FREQUENCY OF A PLATE WITH THREE CRACKS

c/b	$h_a/h_0$				
	0.9	0.8	0.7	0.6	0.5
0.1	1.51561	1.40593	1.29479	1.18186	1.06664
0.3	1.443	1.33958	1.23474	1.12807	1.01897
0.5	1.35095	1.25477	1.15702	1.05716	0.95445
0.7	1.26551	1.17647	1.08552	0.992	0.89496

Figure 8 shows the data in Table VI. When the thickness index ( $\mu = 1 - h_a/h_0$ ) increases, the impregnation becomes thinner, leading to a decrease in frequency. In particular, when  $c/b$  and  $\mu$  increase together, the stiffness of the plate decreases faster, so the frequency decreases very quickly. Figure 9 shows the first four vibration modes of a plate with 3 cracks and  $a = b = 0.5$  m,  $h_a/h_0 = 0.5$ ,  $c/b = 0.7$ , and  $d = 0.25a$ .

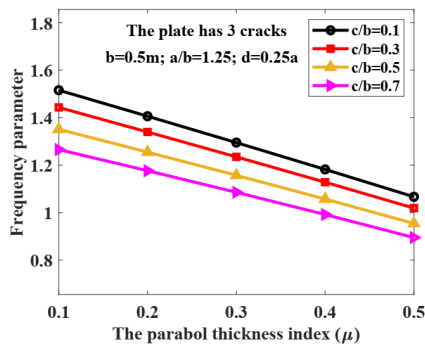


Fig. 8. Relationship between frequency and thickness ratio of the plate with three cracks.

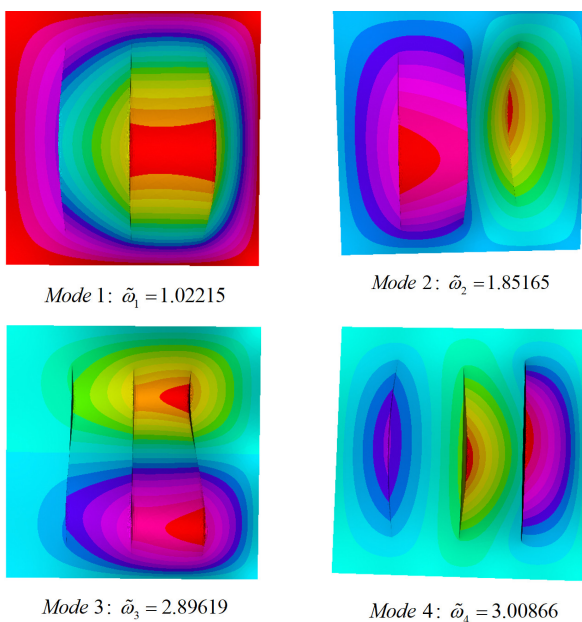


Fig. 9. First four oscillations of parabolic thickness plate with 3 cracks parallel to the y-axis.

The cracks have a significant effect on the frequency and vibration patterns of the plate, as was clearly shown in Figures 5, 7, and 9.

IV. CONCLUSION

This study used the phase-field theory in destructive mechanics and the first-order shear strain theory to study the free vibrations of a plate, whose thickness varies with a parabolic function and has cracks. Numerical results showed that for the case considered: (i) when the crack length is increased, the stiffness of the plate decreases, so the free vibration frequency of the plate will be reduced; (ii) as the number of cracks increases, the free oscillation frequency of the plate decreases; (iii) when the sheet thickness ratio is increased ( $h_a/h_0$ ), the free oscillation frequency of the plate decreases; (iv) when increasing the plate length ratio ( $a/b$ ), the plate is thinner and the vibration frequency decreases. These results would be very helpful when analyzing plate vibrations as cracks propagate over time.

ACKNOWLEDGMENT

This research was funded by the Vietnam Ministry of Education and Training under grant number B2022-GHA-02.

REFERENCES

- [1] K. Akiyama and M. Kuroda, "Fundamental Frequencies of Rectangular Plates with Linearly Varying Thickness," *Journal of Sound and Vibration*, vol. 205, no. 3, pp. 380–384, Aug. 1997, <https://doi.org/10.1006/jsvi.1997.1058>.
- [2] Y. Xiang and C. M. Wang, "Exact Buckling and Vibration Solutions for Stepped Rectangular Plates," *Journal of Sound and Vibration*, vol. 250, no. 3, pp. 503–517, Feb. 2002, <https://doi.org/10.1006/jsvi.2001.3922>.
- [3] I. Shufrin and M. Eisenberger, "Vibration of shear deformable plates with variable thickness — first-order and higher-order analyses," *Journal of Sound and Vibration*, vol. 290, no. 1, pp. 465–489, Feb. 2006, <https://doi.org/10.1016/j.jsv.2005.04.003>.
- [4] M. Saeidifar, S. N. Sadeghi, and M. R. Saviz, "Analytical solution for the buckling of rectangular plates under uni-axial compression with variable thickness and elasticity modulus in the y-direction," *Proceedings of the Institution of Mechanical Engineers, Part C: Journal of Mechanical Engineering Science*, vol. 224, no. 1, pp. 33–41, Jan. 2010, <https://doi.org/10.1243/09544062JMES1562>.
- [5] H. T. Thai and S.-E. Kim, "Levy-type solution for free vibration analysis of orthotropic plates based on two variable refined plate theory," *Applied Mathematical Modelling*, vol. 36, no. 8, pp. 3870–3882, Aug. 2012, <https://doi.org/10.1016/j.apm.2011.11.003>.
- [6] G. Fu, Y. Tuo, B. Sun, C. Shi, and J. Su, "Bending of variable thickness rectangular thin plates resting on a double-parameter foundation: integral transform solution," *Engineering Computations*, vol. 39, no. 7, pp. 2689–2704, Jan. 2022, <https://doi.org/10.1108/EC-11-2021-0692>.
- [7] T. D. Hien, N. D. Hung, N. T. Hiep, G. V. Tan, and N. V. Thuan, "Finite Element Analysis of a Continuous Sandwich Beam resting on Elastic Support and Subjected to Two Degree of Freedom Sprung Vehicles," *Engineering, Technology & Applied Science Research*, vol. 13, no. 2, pp. 10310–10315, Apr. 2023, <https://doi.org/10.48084/etasr.5464>.
- [8] H. T. Duy, N. D. Diem, G. V. Tan, V. V. Hiep, and N. V. Thuan, "Stochastic Higher-order Finite Element Model for the Free Vibration of a Continuous Beam resting on Elastic Support with Uncertain Elastic Modulus," *Engineering, Technology & Applied Science Research*, vol. 13, no. 1, pp. 9985–9990, Feb. 2023, <https://doi.org/10.48084/etasr.5456>.
- [9] D. T. Thuy, L. N. Ngoc, D. N. Tien, and H. V. Thanh, "An Analytical Solution for the Dynamics of a Functionally Graded Plate resting on Viscoelastic Foundation," *Engineering, Technology & Applied Science Research*, vol. 13, no. 1, pp. 9985–9990, Feb. 2023, <https://doi.org/10.48084/etasr.5456>.

- Research, vol. 13, no. 1, pp. 9926–9931, Feb. 2023, <https://doi.org/10.48084/etasr.5420>.
- [10] P. P. Minh and N. D. Duc, "The effect of cracks on the stability of the functionally graded plates with variable-thickness using HSDT and phase-field theory," *Composites Part B: Engineering*, vol. 175, Art. no. 107086, Oct. 2019, <https://doi.org/10.1016/j.compositesb.2019.107086>.
- [11] P. P. Minh and N. D. Duc, "The effect of cracks and thermal environment on free vibration of FGM plates," *Thin-Walled Structures*, vol. 159, Feb. 2021, Art. no. 107291, <https://doi.org/10.1016/j.tws.2020.107291>.
- [12] P. P. Minh, D. T. Manh, and N. D. Duc, "Free vibration of cracked FGM plates with variable thickness resting on elastic foundations," *Thin-Walled Structures*, vol. 161, Apr. 2021, Art. no. 107425, <https://doi.org/10.1016/j.tws.2020.107425>.
- [13] N. D. Duc and P. P. Minh, "Free vibration analysis of cracked FG CNTRC plates using phase field theory," *Aerospace Science and Technology*, vol. 112, May 2021, Art. no. 106654, <https://doi.org/10.1016/j.ast.2021.106654>.
- [14] P. P. Minh, "Analysis free vibration of the functionally grade material cracked plates with varying thickness using the Phase-field theory," *Transport and Communications Science Journal*, vol. 70, no. 2, pp. 122–131, 2019, <https://doi.org/10.25073/tcsj.70.2.35>.
- [15] Minh P. P., "Using phase field and third-order shear deformation theory to study the effect of cracks on free vibration of rectangular plates with varying thickness," *Transport and Communications Science Journal*, vol. 71, no. 7, pp. 853–867, 2020, <https://doi.org/10.47869/tcsj.71.7.10>.
- [16] V. A. Le, M. P. Pham, and T. A. Bui, "Stability of Cracked Plates with Nonlinearly Variable Thickness Resting on Elastic Foundations," *Journal of Materials and Engineering Structures*, vol. 9, no. 4, pp. 641–651, Dec. 2022.
- [17] C. S. Huang, P. J. Yang, and M. J. Chang, "Three-dimensional vibration analyses of functionally graded material rectangular plates with through internal cracks," *Composite Structures*, vol. 94, no. 9, pp. 2764–2776, Sep. 2012, <https://doi.org/10.1016/j.compstruct.2012.04.003>.